F-18-Glyco-RGD Peptides for PET Imaging of Integrin Expression: Efficient Radiosynthesis by Click Chemistry and Modulation of Biodistribution by Glycosylation

ARTICLE *in* MOLECULAR PHARMACEUTICS · DECEMBER 2013

Impact Factor: 4.38 · DOI: 10.1021/mp4004817 · Source: PubMed

molecular pharmaceutics

Article

pubs.acs.org/molecularpharmaceutics

^{18}F-Glyco-RGD Peptides for PET Imaging of Integrin Expression: Efficient Radiosynthesis by Click Chemistry and Modulation of Biodistribution by Glycosylation

Simone Maschauer,[†] Roland Haubner,[‡] Torsten Kuwert,[†] and Olaf Prante*,[†]

[†]Department of Nuclear Medicine, Molecular Imaging and Radiochemistry, Friedrich Alexander University, 91054 Erlangen, Germany

[‡]Department of Nuclear Medicine, Innsbruck Medical University, 6020 Innsbruck, Austria

Supporting Information

ABSTRACT: Glycosylation frequently improves the biokinetics and clearance properties of macromolecules *in vivo* and could therefore be used for the design of radiopharmaceuticals for positron emission tomography (PET). Recently, we have developed a click chemistry method for ^{18}F-fluoroglycosylation of alkyne-bearing RGD-peptides targeting the integrin receptor. To investigate whether this strategy could yield an ^{18}F-labeled RGD glycopeptide with favorable biokinetics, we generated a series of new RGD glycopeptides, varying the 6-fluoroglycosyl residue from monosaccharide to disaccharide units, which provided the glucosyl ([^{19}F]6Glc-RGD, **4b**), galactosyl ([^{19}F]Gal-RGD, **4c**), maltosyl ([^{19}F]Mlt-RGD, **4e**), and cellobiosyl ([^{19}F]Cel-RGD, **4f**) conjugated peptides in high yields and purities of >97%. All of these RGD glycopeptides showed high affinity to $\alpha_v\beta_3$ (11−55 nM), $\alpha_v\beta_5$ (6−14 nM), and to $\alpha_v\beta_3$-positive U87MG cells (90−395 nM). ^{18}F-labeling of the various carbohydrate precursors (**1a**−**f**) using cryptate-assisted reaction conditions (CH_3CN, 85 °C, 10 min) gave ^{18}F-labeled glycosyl azides in radiochemical yields (RCYs) of up to 84% ([^{18}F]**2b**). The deacetylation and subsequent click reaction with the alkyne-bearing cyclic RGD peptide proceeded in one-pot reactions with RCYs as high as 81% in 15−20 min at 60 °C, using a minimal amount of peptide precursor (100 nmol). Optimization of the radiosynthesis strategy gave a decay-uncorrected RCY of 16−24% after 70−75 min (based on [^{18}F]fluoride). Due to their high-yield radiosyntheses, the glycopeptides [^{18}F]6Glc-RGD and [^{18}F]Mlt-RGD were chosen for comparative biodistribution studies and dynamic small-animal PET imaging using U87MG tumor-bearing nude mice. [^{18}F]6Glc-RGD and [^{18}F]Mlt-RGD showed significantly decreased liver and kidney uptake by PET relative to the 2-[^{18}F]fluoroglucosyl analog [^{18}F]2Glc-RGD, and showed specific tumor uptake *in vivo*. Notably, [^{18}F]Mlt-RGD revealed uptake and retention in the U87MG tumor comparable to that of [^{18}F]Galacto-RGD. Both [^{18}F]6Glc-RGD and [^{18}F]Mlt-RGD were obtained by a reliable and easy click chemistry-based procedure, much more rapidly than was [^{18}F]Galacto-RGD. Due to its favorable biodistribution and tissue clearance *in vivo*, [^{18}F]Mlt-RGD represents a viable alternative radiotracer for imaging integrin expression in solid tumors by PET.

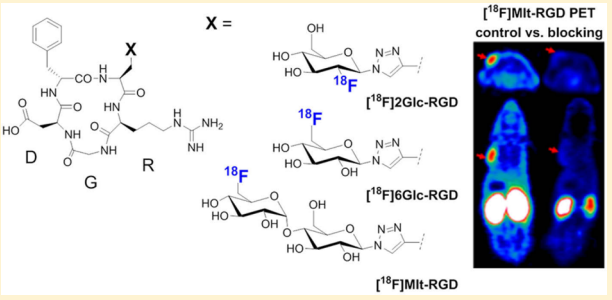

KEYWORDS: *RGD peptide, fluorine-18, glycosylation, click chemistry, positron emission tomography*

INTRODUCTION

The molecular mechanisms underlying angiogenesis have been the subject of intensive research in the last few decades.[1] These efforts have led to considerable knowledge of the role of angiogenesis and its disturbances in the pathogenesis of diseases such as macular degeneration, and notably in solid tumors. These insights have led to the development and validation of new therapeutic drugs interfering with angiogenesis.[2] Moreover, efforts have been expended in developing radiopharmaceuticals for molecular imaging of processes pertinent to the formation of new vessels.[3] Angiogenesis tracers for positron emission tomography (PET) have the potential to diagnose foci of inflammation or tumor deposits and could also be used clinically for rational selection of patients for antiangiogenic therapies and for monitoring effects of treatment in individualized therapy.

One class of PET angiogenesis tracer is based on RGD containing peptides which target the integrin $\alpha_v\beta_3$, a receptor, which plays a major role during angiogenesis by mediating adhesion between endothelial cells. One approach relies on the pioneering work by Kessler et al., who successfully developed cyclic pentameric RGD-containing peptide inhibitors with high specificity and affinity for this integrin.[4] These efforts have yielded a number of radiolabeled RGD derivatives for imaging

Received: August 14, 2013
Revised: October 25, 2013
Accepted: December 10, 2013

dx.doi.org/10.1021/mp4004817 | *Mol. Pharmaceutics* XXXX, XXX, XXX−XXX

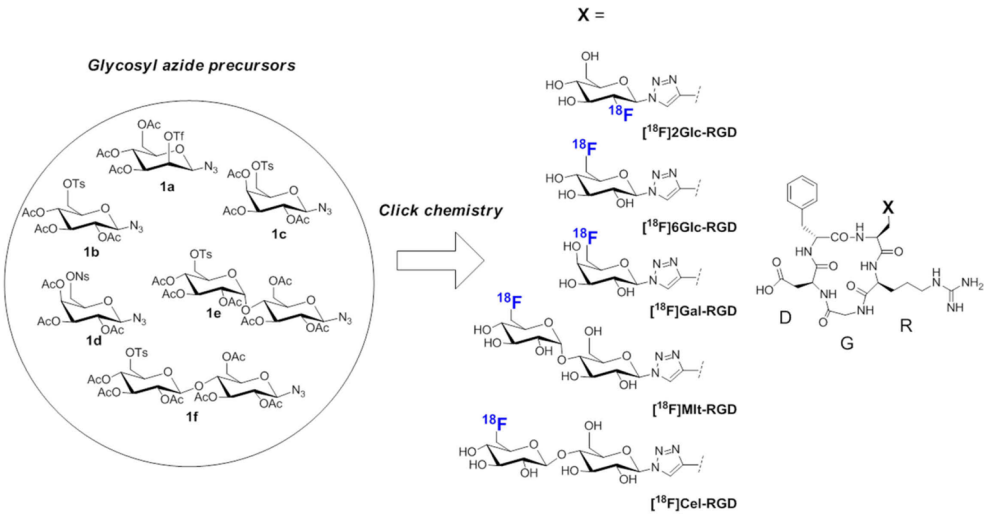

Figure 1. Synthetic route toward a series of ^{18}F-labeled RGD glycopeptides following a click chemistry-based strategy by the use of a small library of glycosyl azide precursors.

$\alpha_v\beta_3$ expression in tumors and nontumor tissues.[5] Very recently, Al[^{18}F]F-NOTA-PRGD2 ([^{18}F]alfatide) has been produced using fluoride-aluminum complex chemistry, and has entered clinical studies.[6] The glycoconjugate [^{18}F]Galacto-RGD has also been applied in various clinical PET studies, including patients with malignant melanoma, glioblastoma, head and neck cancer, breast cancer, sarcoma, nonsmall cell lung cancer, and prostate cancer.[7−9] These studies demonstrated beneficial pharmacokinetics and *in vivo* clearance properties of [^{18}F]Galacto-RGD, that is, rapid, predominately renal tracer elimination, resulting in low background radioactivity in almost all organs, and consequently with tumor-to-background ratios favoring the detection of lesions. Excellent PET imaging properties have also been reported for other glycopeptides and glycoconjugates, including octreotide analogues and, more recently, nonpeptide tracers.[8,10,11] However, the accessibility of [^{18}F]Galacto-RGD has been hitherto hampered by its time-consuming multistep radiosynthesis; a more reliable ^{18}F-synthesis for a RGD-based glycopeptide is still needed.

Recently developments in so-called "click chemistry" have provided improved strategies for ^{18}F-labeling, taking advantage of the speed, reliability, and selectivity of these reactions.[12] The most prominent example of a click chemistry reaction is the copper(I)-catalyzed azide−alkyne cycloaddition (CuAAC), which is a highly chemo- and regioselective and high-yielding reaction.[13,14] Only a limited number of click chemistry-based radiosyntheses of ^{18}F-labeled glycopeptides have been described, including the oxime formation of aminooxy-functionalized peptides with 4-[^{18}F]fluorobenzaldehyde or 2-deoxy-2-[^{18}F]fluoroglucose ([^{18}F]FDG)[15−17] and the use of thiol-reactive glycosyl donors derived from [^{18}F]FDG.[18,19]

Recently, we developed a strategy for concomitant ^{18}F-labeling and glycosylation of alkyne-bearing molecules using CuAAC click chemistry.[20,21] Meanwhile, this ^{18}F-click glycosylation method has been successfully adapted by others to the radiosyntheses of ^{18}F-glycoproteins and nonpeptide glycoconjugates.[11,22] We applied this strategy to the radiosynthesis of a glucosylated cyclic RGD peptide ([^{18}F]2Glc-RGD) that was successfully used for imaging of $\alpha_v\beta_3$ integrin expression in a mouse model.[21] However, the biodistribution of this tracer suffered from clearance properties in liver and kidney that were inferior to the pharmacokinetics of [^{18}F]galacto-RGD, which had relatively rapid washout from nontumor tissues.

The aim of this study was to develop an ^{18}F-labeled RGD glycopeptide with improved pharmacokinetic properties by varying the ^{18}F-labeled glycosyl residue. We predicted that this might be achieved by aiming at suitable glycosyl precursors for the introduction of 6-deoxy-6-[^{18}F]fluorogalactosyl, 6-deoxy-6-[^{18}F]fluoroglucosyl, 6′-deoxy-6′-[^{18}F]fluoromaltosyl, and 6′-deoxy-6′-[^{18}F]fluorocellobiosyl residues to the RGD motif (Figure 1). Clickable ^{18}F-glycosyl azides should facilitate and simplify the radiosynthesis of ^{18}F-labeled glycopeptides. Therefore, we synthesized a series of novel 6-*O*-sulfonylglycosyl azides as ^{18}F-labeling precursors (Figure 1): 2,3,4-tri-*O*-acetyl-6-*O*-toluenesulfonyl-*β*-D-glucopyranosyl azide **1b**, 2,3,4-tri-*O*-acetyl-6-*O*-toluenesulfonyl-*β*-D-galactopyranosyl azide **1c**, 2,3,4-tri-*O*-acetyl-6-*O*-(2-nitrophenyl)sulfonyl-*β*-D-galactopyranosyl azide **1d**, 2′,3′,4′,2,3,6-hexa-*O*-acetyl-6′-*O*-toluenesulfonyl-*β*-D-maltosyl azide **1e**, and 2′,3′,4′,2,3,6-hexa-*O*-acetyl-6′-*O*-toluenesulfonyl-*β*-D-cellobiosyl azide **1f** and studied their applicability as ^{18}F-labeling precursors compared with the 2-triflate precursor **1a** previously developed in our laboratory.[20] We then tested our series of ^{18}F-glycosyl azides for click labeling of the alkyne-bearing cyclic RGD peptide c(RGDfPra) to provide the series of RGD glycopeptides [^{18}F]6Glc-RGD, [^{18}F]Gal-RGD, [^{18}F]Mlt-RGD, and [^{18}F]Cel-RGD (Figure 1). In addition, we measured affinities of the resulting ^{18}F-glyco-RGD peptides to $\alpha_v\beta_3$ and $\alpha_v\beta_5$ integrin receptors and characterized the influence of heteroglycosylation on the biodistribution and clearance properties *in vivo* in small animal PET studies of tumor-bearing nude mice.

EXPERIMENTAL SECTION

General. All chemicals and reagents were of analytical grade and obtained from commercial sources unless stated otherwise. Analytical high-performance liquid chromatography (HPLC) was performed on an Agilent 1100 system with a quarternary pump and variable wavelength detector and radio-HPLC detector D505TR (Canberra Packard). Computer analysis of the HPLC data was performed using FLO-One software (Canberra Packard). Electron-spray ionization (ESI) mass spectrometry analysis was performed using a Bruker Esquire 2000 instrument. The carbohydrate syntheses of the glycosyl

dx.doi.org/10.1021/mp4004817 | *Mol. Pharmaceutics* XXXX, XXX, XXX−XXX

labeling precursors **1e** and **1f**, all intermediates and precursors for the syntheses of the reference RGD peptides [^{19}F]6Glc-RGD (**4b**), [^{19}F]Gal-RGD (**4c**), [^{19}F]Mlt-RGD (**4e**), and [^{19}F]Cel-RGD (**4f**), and their analytical data are given in the Supporting Information file (see associated content). The syntheses of **1a**, **2a**, **3a**, **4a** and [^{18}F]**2a**, [^{18}F]**3a**, and [^{18}F]**4a** were performed as previously described.[20,21]

2,3,4-Tri-*O*-acetyl-6-*O*-*p*-toluenesulfonyl-β-D-glucopyranosyl Azide (1b). To a solution of *p*-toluenesulfonyl chloride (3.2 g, 16.7 mmol) in anhydrous pyridine (45 mL) at 0 °C D-glucose (3 g, 16.7 mmol) was added. The solution was stirred overnight at 0 °C. Subsequently, acetic anhydride (13.2 mL) was added dropwise. The solution was allowed to warm to room temperature, and after 1 h the solvent was removed *in vacuo*. The residue was dissolved in dichloromethane, and the solution was washed several times with saturated $NaHCO_3$, 0.2 M HCl, and water, dried with Na_2SO_4, and concentrated again to afford the crude 1,2,3,4-tetra-*O*-acetyl-6-*O*-*p*-toluenesulfonyl-β-D-glucopyranose **7b** which was crystallized from ethanol: 3 g, 6.0 mmol, 36% yield. ^{1}H NMR (600 MHz, $CHCl_3$): δ ppm 1.99 (s, 3H, OAc), 2.00 (s, 3H, OAc), 2.02 (s, 3H, OAc), 2.09 (s, 3H, OAc), 2.46 (s, 3H, CH_3-Ts), 3.84 (ddd, *J* = 10.07, 4.55, 2.87 Hz, 1H, H-5), 4.15 (dd, *J* = 11.17, 2.89 Hz, 1H, H-6b), 4.11 (dd, *J* = 11.21, 4.59 Hz, 1H, H-6a), 5.04 (dd (t), *J* = 9.5 Hz, 1H, H-4), 5.05 (dd, *J* = 9.41, 8.23 Hz, 1H, H-2), 5.20 (t, *J* = 9.37 Hz, 1H, H-3), 5.65 (d, *J* = 8.19 Hz, 1H, H-1), 7.35 (d, *J* = 7.97 Hz, 2H), 7.77 (d, *J* = 8.29 Hz, 2H). ^{13}C NMR (151 MHz, $CHCl_3$): δ ppm 170.09, 169.27, 169.12, 168.75 (4x C═O, OAc), 145.14 (Ts), 132.43 (Ts), 129.86 (2C, Ts), 128.17 (2C, Ts), 91.53 (C-1), 72.60, 72.17, 70.05, 67.95, 66.74 (C-2 − C-6), 21.68 (CH_3, Ts), 20.74, 20.55, 20.52, 20.49 (4x CH_3, OAc).

To a solution of 1,2,3,4-tetra-*O*-acetyl-6-*O*-*p*-toluenesulfonyl-β-D-glucopyranose **7b** (3 g, 6 mmol) in dichloromethane (20 mL) HBr (33% in acetic acid, 30 mL) was added dropwise at 0 °C, and the solution was stirred for 3 h at room temperature. The mixture was diluted with dichloromethane (150 mL) and washed with saturated $NaHCO_3$ (3 × 50 mL), water (2 × 50 mL), dried with Na_2SO_4 and concentrated *in vacuo*. The crude product was purified by column chromatography (EtOAc-*n*-hexan 1:1) to afford 2,3,4-tri-*O*-acetyl-6-*O*-*p*-toluenesulfonyl-β-D-glucopyranosyl bromide as a yellow oil (2.8 g, 5.3 mmol, 88% yield) that was dissolved in in EtOAc (30 mL) and tetrabutylammonium hydrogen sulfate (1.8 g, 5.3 mmol) and sodium azide (1.4 g, 21.2 mmol), and saturated $NaHCO_3$ (30 mL) was added. The two-phase mixture was vigorously stirred for 2 h at room temperature; EtOAc (70 mL) was added, and the organic phase was washed with saturated $NaHCO_3$ (2 × 50 mL) and brine (50 mL). After drying with Na_2SO_4 and evaporation of the solvent, the crude product **1b** was recrystallized twice from EtOH: 1.8 g, 3.8 mmol, yield 70%. ^{1}H NMR (600 MHz, $CDCl_3$): δ ppm 1.99 (s, 3H, OAc), 2.02 (s, 3H, OAc), 2.06 (s, 3H, OAc), 2.46 (s, 3H, CH_3-Ts), 3.83 (ddd, *J* = 10.10, 5.70, 2.66 Hz, 1H, H-5), 4.09 (dd, *J* = 11.24, 5.72 Hz, 1H, H-6a), 4.15 (dd, *J* = 11.24, 2.65 Hz, 1H, H-6b), 4.56 (d, *J* = 8.87 Hz, 1H, H-1), 4.85 (t, *J* = 9.26 Hz, 1H, H-2), 4.95 (t, *J* = 9.77 Hz, 1H, H-4), 5.18 (t, *J* = 9.50 Hz, 1H, H-3), 7.37 (d, *J* = 8.08 Hz, 2H, Ts), 7.79 (d, *J* = 8.29 Hz, 2H, Ts). ^{13}C NMR (151 MHz, $CDCl_3$): δ ppm 170.04, 169.32, 169.11 (3× C═O, OAc), 145.33 (Ts), 132.25 (Ts), 129.94 (2C, Ts), 128.13 (2C, Ts), 87.69 (C-1), 73.65, 72.34, 70.40, 68.14, 67.21 (C-2−C-6), 21.69 (CH_3, Ts), 20.53, 20.51, 20.50 (3× CH_3, OAc). ESI-MS: *m*/*z* = 508.1 $[M + Na]^+$.

2,3,4-Tri-*O*-acetyl-6-*O*-*p*-toluenesulfonyl-β-D-galactopyranosyl Azide (1c). The synthesis was performed according to the procedure described in the literature.[23] To a solution of *p*-toluenesulfonyl chloride (465 mg, 2.44 mmol) in anhydrous pyridine (7 mL) at 0 °C β-galactosyl azide (500 mg, 2.44 mmol; Sigma-Aldrich) was added, and the solution was stirred overnight at 0 °C. Acetic anhydride (2 mL) was added dropwise at 0 °C and the solution was stirred for 1 h. The solution was diluted with dichloromethane, and the organic phase was washed several times with saturated $NaHCO_3$, 0.2 M HCl, and water, dried with Na_2SO_4, and concentrated to afford the crude product **1c** which was crystallized from absolute EtOH: 350 mg, 730 μmol, 30% yield. ^{1}H NMR (600 MHz, $CDCl_3$): δ ppm 1.97 (s, 3H), 2.07 (s, 3H), 2.08 (s, 3H), 2.46 (s, 3H), 4.03 (m, 2H, H-5, H-6a), 4.13 (dd, *J* = 9.42, 5.73 Hz, 1H, H-6b), 4.55 (d, *J* = 8.77 Hz, 1H, H-1), 5.00 (dd, *J* = 10.37, 3.37 Hz, 1H, H-3), 5.10 (dd, *J* = 10.37, 8.77 Hz, 1H, H-2), 5.40 (dd, *J* = 3.33, 0.71 Hz, 1H, H-4), 7.38−7.35 (m, 2H), 7.79−7.76 (m, 2H). ^{13}C NMR (151 MHz, $CDCl_3$): δ ppm 169.83, 169.80, 169.32, 145.38, 132.20, 130.02, 128.07, 88.24, 72.73, 70.49, 67.84, 66.66, 65.98, 21.69, 20.65, 20.48.

2,3,4-Tri-*O*-acetyl-6-*O*-*p*-nitrobenzenesulfonyl-β-D-galactopyranosyl Azide (1d). 1d was synthesized starting from β-galactosyl azide (500 mg, 2.44 mmol) following the protocol described for **1c** but using *p*-nitrobenzenesulfonyl chloride (540 mg, 2.44 mmol) instead of *p*-toluenesulfonyl chloride. **1d** was obtained after column chromatography (toluene−EtOAc 1:1) as an off-white solid in a yield of 40% (500 mg, 970 μmol). ^{1}H NMR (360 MHz, $CDCl_3$): δ ppm 1.98 (s, 3H), 2.08 (s, 3H), 2.12 (s, 3H), 4.07 (ddd, *J* = 6.77, 5.40, 1.20 Hz, 1H, H-5), 4.20 (dd, *J* = 10.53, 5.39 Hz, 1H, H-6), 4.22 (dd, *J* = 10.52, 6.88 Hz, 1H, H-6), 4.56 (d, *J* = 8.68 Hz, 1H, H-1), 5.01 (dd, *J* = 10.37, 3.32 Hz, 1H, H-3), 5.11 (dd, *J* = 10.46, 8.63 Hz, 1H, H-2), 5.41 (dd, *J* = 3.31, 1.11 Hz, 1H, H-4), 8.44−8.40 (m, 2H), 8.13−8.09 (m, 2H). ^{13}C NMR (90.56 MHz, $CDCl_3$): δ ppm 169.91, 169.84, 169.26, 151.08, 141.08, 129.40, 124.58, 88.26, 72.67, 70.42, 67.72, 67.24, 66.68, 20.62, 20.53, 20.46. ESI-MS (*m*/*z*): = 539.0 $[M + Na]^+$, *m*/*z* = 555.0 $[M + K]^+$.

Syntheses of Reference Compounds 4b, 4c, 4e, or 4f. To a solution of 6-deoxy-6-fluoro-D-glucopyranosyl azide (**3b**) (1.86 mg, 2.4 μmol), 6-deoxy-6-fluoro-D-galactopyranosyl azide (**3c**) (1.86 mg, 2.4 μmol), 6′-deoxy-6′-fluoro-β-maltosyl azide (**3e**) (2.25 mg, 2.4 μmol), or 6′-deoxy-6′-fluoro- β-cellobiosyl azide (**3f**) (2.25 mg, 2.4 μmol) and c(RGDfPra)[21] (1.37 mg, 2.4 μmol) in a solution of phosphate-buffered saline (PBS; 10% ethanol) (0.5 mL), a solution of copper(II)sulfate pentahydrate (0.2 M, 10 μL) and a solution of sodium ascorbate (0.6 M, 10 μL) were added. The mixture was stirred at room temperature for 30 min, then diluted with water/acetonitrile (9:1, 0.5 mL), and subjected to semipreparative RP-HPLC for purification of the desired product (Kromasil C8, 125 × 8 mm, 10−40% acetonitrile (0.1% trifluoroacetic acid, TFA) in water (0.1% TFA) in a linear gradient over 30 min, 4 mL/min, t_R(**4b**) = 11.0 min, t_R(**4c**) = 9.3 min, t_R(**4e**) = 7.5 min, t_R(**4f**) = 6.4 min). After lyophilization of the product fraction, the glycopeptides were obtained as white solids in yields of 70−80%. ESI-MS: **4b**: *m*/*z* = 778.4 $[M + H]^+$; **4c**: *m*/*z* = 778.4 $[M + H]^+$; **4e**: *m*/*z* = 940.6 $[M + H]^+$; **4f**: *m*/*z* = 940.4 $[M + H]^+$, 481.7 $[M + H + Na]^{2+}$.

Synthesis of c(RGDfPra). The peptide was synthesized using Fmoc-protocols as described previously.[21]

dx.doi.org/10.1021/mp4004817 | *Mol. Pharmaceutics* XXXX, XXX, XXX−XXX

Production of [^{18}F]fluoride. No-carrier-added (n.c.a.) [^{18}F]fluoride was produced by the ^{18}O(p,n)^{18}F reaction on ^{18}O-enriched water (>98%, Rotem Ind. LTD) using a proton beam of 11 MeV generated by a RDS 111 cyclotron (Siemens/CTI; Pet Net GmbH, Erlangen).

^{18}F-Labeling under "Mild" Reaction Conditions. A QMA-cartridge with [^{18}F]fluoride was eluted with a solution of 10 mg of Kryptofix 2.2.2, 0.1 M K_2CO_3 (17.5 μL), and 0.1 M KH_2PO_4 (17.5 μL) in 1 mL of acetonitrile/water (8:2). The solution was evaporated using a stream of nitrogen at 85 °C and coevaporated to dryness with CH_3CN (2 × 500 μL). The respective labeling precursor (**1a**, **1b**, **1c**, **1d**, **1e**, or **1f**, 15 μmol) in anhydrous acetonitrile (450 μL) was added, and the solution was stirred for 10 min at 85 °C. Samples were withdrawn from the reaction mixture for the analysis of the radiochemical yields of the corresponding ^{18}F-labeled glycosyl azides [^{18}F]**2b**, [^{18}F]**2c**, [^{18}F]**2e**, and [^{18}F]**2f** by radio-HPLC (Figure S1). The ^{18}F-labeled products were identified by retention time (t_R) on the radio-HPLC system and by coinjection of the corresponding reference compounds (Kromasil C8, 250 × 4.6 mm, 40−100% acetonitrile (0.1% TFA) in water (0.1% TFA) in a linear gradient over 50 min, 1.5 mL/min, t_R (**2b**) = 9.2 min, t_R (**2c**) = 9.4 min, t_R (**2e**) = 14.3 min, t_R (**2f**) = 13.4 min).

Radiosynthesis of [^{18}F]6Glc-RGD ([^{18}F]4b), [^{18}F]Gal-RGD ([^{18}F]4c), or [^{18}F]Mlt-RGD ([^{18}F]4e). Acetylated glycosyl azides [^{18}F]**2b**, [^{18}F]**2c**, or [^{18}F]**2e** were isolated by evaporating the solvent in a stream of nitrogen, dissolving the residue with acetonitrile/water (30:70, 500 μL), and separation by semi-preparative HPLC (Kromasil C8, 125 × 8 mm, 4 mL/min, acetonitrile (0.1% TFA)/water (0.1% TFA) 30−70% in 30 min). The product fraction was diluted with water (1:10), transferred to a C18-cartridge (Merck, 100 mg), dried in a stream of nitrogen, and eluted with ethanol (1 mL). [^{18}F]**2b**, [^{18}F]**2c**, or [^{18}F]**2e** was dried at 60 °C in a stream of nitrogen, and subsequently NaOH (250 μL, 60 mM, 10% ethanol) was added. The deacetylation was complete after stirring for 5 min at 60 °C, and the crude product [^{18}F]**3b**, [^{18}F]**3c**, or [^{18}F]**3e** was used for the click reaction with the alkyne in a one-pot procedure. This was accomplished by neutralizing the solution with HCl (1 N, 13.5 μL), followed by addition of c(RGDfPra) (100 μg, dissolved in ethanol/water (260 μL, 1:1)), $CuSO_4$ (0.2 M, 10 μL), and sodium ascorbate (0.6 M, 10 μL). The reaction mixture was stirred for 15−20 min at 60 °C. The radiochemical yield was 81% for [^{18}F]**4b**, 36% for [^{18}F]**4c**, and 80% for [^{18}F]**4e** as determined by analytical HPLC from a sample withdrawn from the reaction mixture. t_R ([^{18}F]**4b**) = 1.57 min, t_R ([^{18}F]**4c**) = 1.37 min, t_R ([^{18}F]**4e**) = 1.10 min (radio-HPLC: Chromolith C8, 10 × 4.6 mm, 10−50% acetonitrile (0.1% TFA) in water (0.1% TFA) in a linear gradient over 5 min, 4 mL/min). ^{18}F-glycopeptides [^{18}F]**4b**, [^{18}F]**4c**, or [^{18}F]**4e** were isolated by semipreparative HPLC (Kromasil C8, 125 × 8 mm, 4 mL/min t_R ([^{18}F]**4b**) = 11.0 min, t_R ([^{18}F]**4c**) = 9.3 min, t_R ([^{18}F]**4e**) = 7.5 min (10−40% acetonitrile (0.1% TFA) in water (0.1% TFA) in a linear gradient over 30 min). The product fraction was diluted in water and passed through a RP-18 cartridge (Lichrolut 100 mg, Merck), and the product was eluted with a solution of ethanol/PBS (1:1, 800 μL). For *in vitro* and *in vivo* experiments the solvent was evaporated *in vacuo*, and the ^{18}F-glycopeptides were formulated with PBS (pH 7.4). Starting from [^{18}F]fluoride (500 MBq), this procedure yielded 80−120 MBq (16−24% decay-uncorrected radiochemical yield) of [^{18}F]**4b** or [^{18}F]**4e** in a total synthesis time of 70−75 min.

Stability in Serum *in Vitro*. An aliquot of the ^{18}F-labeled glycopeptide [^{18}F]**4b** or [^{18}F]**4e** in PBS (35 μL) was added to human serum (200 μL) and incubated at 37 °C. Aliquots (25 μL) were taken at various time intervals (5−60 min) and quenched in methanol/water (1:1, 100 μL). The samples were centrifuged, and the supernatants were analyzed by radio-HPLC.

Determination of the Partition Coefficients (log *D*). The lipophilicity of the ^{18}F-labeled radioligands was assessed by determination of the water−octanol partition coefficient. 1-Octanol (0.5 mL) was added to a solution of approximately 25 kBq of the ^{18}F-labeled compound in PBS (0.5 mL, pH 7.4) ,and the layers were vigorously mixed for 3 min at room temperature. The tubes were centrifuged (14000 rpm, 1 min) and three samples of each layer (each 100 μL) were counted in a γ-counter (Wallac Wizard). The partition coefficient was determined by calculating the ratio cpm (octanol)/cpm (PBS) and expressed as log $D_{7.4}$ = log($cpm_{octanol}/cpm_{PBS}$). The experiments were performed in triplicate and data reported as mean (±SD).

Cell Culture. The human $\alpha_v\beta_3$-expressing glioblastoma cell line U87MG (ECACC no. 89081402) was grown in DMEM supplemented with nonessential amino acids (1%), sodium pyruvate (1 mM), and FBS (10%) at 37 °C in a humidified atmosphere of 5% CO_2 as described previously.[18] The cells were routinely subcultured every 4 days. Routine test of the U87MG cells for contamination with mycoplasma were always negative.

$\alpha_v\beta_3$ and $\alpha_v\beta_5$ Solid-Phase Receptor Binding Assay. The receptor binding assay was performed following the procedure described previously.[18] In brief, commercially available purified $\alpha_v\beta_3$ or $\alpha_v\beta_5$ (Triton-X solution, Chemicon International) was diluted at 250 ng/mL or 500 ng/mL, respectively, in coating buffer (25 mM Tris-HCl, 150 mM NaCl, 1 mM $CaCl_2$, 0.5 mM $MgCl_2$, 1 mM $MnCl_2$, pH 7.4), and an aliquot of 100 μL/well was added to a 96-well microtiter plate (Maxisorb, Nunc, Wiesbaden, Germany) and incubated at 4 °C overnight. The wells were washed once with blocking buffer (200 μL, coating buffer containing 1% (w/v) BSA) and incubated for two hours with blocking buffer (200 μL) at room temperature. The plate was rinsed twice with binding buffer (coating buffer with 0.1% (w/v) BSA) and incubated in the presence of the competing ligand (90 μL, 0.5 pM to 500 nM echistatin; 0.05 nM to 50 μM RGD peptide in binding buffer) with [^{125}I]echistatin (0.37 kBq/well, 10 μL, 0.05 nM; PerkinElmer, Germany). After incubation for 3 h, the wells were washed three times with binding buffer, and bound [^{125}I]echistatin was solubilized with warm NaOH (2 M). The radioactivity in the resulting samples was measured by a γ-counter (Wallac Wizard). Each data point represents the mean from three wells. All measurements were repeated at least two times. K_i values were calculated by the use of the software program GraphPad PRISM (GraphPad Software Inc., CA, USA), employing the algorithm for "heterologous competitive binding with ligand depletion".

Cell Binding Assay. U87MG cells were harvested, suspended in growth media, and seeded in 96-well plates at a concentration of 500 000 cells per well (200 μL). The 96-well plates were centrifuged at 150 g for 2 min; the supernatant was removed by aspiration, and cells were suspended in blocking buffer (25 mM Tris-HCl, 150 mM NaCl, 1 mM $CaCl_2$, 0.5 mM

dx.doi.org/10.1021/mp4004817 | *Mol. Pharmaceutics* XXXX, XXX, XXX−XXX

$MgCl_2$, 1 mM $MnCl_2$, pH 7.4, 1% BSA). The plates were centrifuged again at 150 g for 2 min, and the supernatant was removed. After incubation of the cell suspension with blocking buffer for 15 min at room temperature, centrifugation was repeated, and the cell pellets were washed twice with binding buffer. Subsequently, the cells were incubated on a shaker in the presence of varied amounts of competing ligand (90 μL, 0.05 nM to 50 μM RGD peptide) with 370 Bq/Eppendorf tube [^{125}I]echistatin (10 μL, 0.5 nM) in a total volume of 100 μL of binding buffer (25 mM Tris-HCl, 150 mM NaCl, 1 mM $CaCl_2$, 0.5 mM $MgCl_2$, 1 mM $MnCl_2$, pH 7.4, 0.1% BSA). After the incubation time of 1 h cells were rinsed twice with binding buffer, and the supernatant was removed; the cell pellets with bound [^{125}I]echistatin were resuspended in 2 N NaOH (200 μL) and transferred in counting tubes for measuring the radioactivity with a γ-counter (Wallac Wizard). Each data point is the mean of three determinations. All measurements were repeated at least twice. K_i values were calculated as above.

Animal Model. All animal experiments were performed in compliance with the protocols approved by the local Animal Protection Authorities (Regierung Mittelfranken, Germany, no. 54-2532.1-15/08). Athymic nude mice (nu/nu) were obtained from Harlan Winkelmann GmbH (Borchen, Germany) at 9–11 weeks of age and were kept under standard conditions (12 h light/dark) with food and water available ad libitum. U87MG cells were harvested and suspended in sterile PBS at a concentration of 2×10^7 cells/mL. Viable cells (2×10^6) in PBS (100 μL) were injected subcutaneously in the back. One to two weeks after inoculation the mice, now weighing about 40 g and bearing tumors of 400–800 mg, were used for biodistribution and small-animal PET studies.

Biodistribution Studies. U87MG xenografted mice were injected with [^{18}F]6Glc-RGD ([^{18}F]**4b**) or ^{18}F-Mlt-RGD ([^{18}F]**4e**) to a tail vein (4–10 MBq/mouse). The animals were killed by cervical dislocation 30, 60, or 120 min postinjection (p.i.). The tumors, other tissues (lung, liver, kidneys, heart, brain, muscle, and intestine), and blood were removed and weighed. Radioactivity of the samples was measured using a γ-counter and expressed as percentage of injected dose per gram of tissue (%ID/g), from which we calculated tumor-to-organ ratios. The blockade experiment was carried out by coinjecting randomly chosen mice with 500 μg (c(RGDfK)) (12.5 mg/kg body weight) together with the radiotracer. These mice were killed by cervical dislocation at 65 min p.i., and organs and tissue were removed, weighed, and counted as described above.

Small-Animal PET Imaging. PET scans and image analysis were performed using a small-animal PET scanner (Inveon, Siemens Medical Solutions). About 3–15 MBq of [^{18}F]6Glc-RGD ([^{18}F]**4b**) or [^{18}F]Mlt-RGD ([^{18}F]**4e**) were intravenously injected into each mouse (n = 3–5) under isoflurane anesthesia (4%). Thereupon, a 60-min dynamic emission scan (12 × 10 s, 3 × 1 min, 5 × 5 min, 3 × 10 min, total of 23 frames) was initiated. After iterative maximum *a posteriori* (MAP) image reconstruction of the decay and attenuation corrected images, regions of interest (ROIs) were drawn over the tumor and other targets. The radioactivity concentration within the tumor region was obtained from the mean value within the multiple ROIs and then converted to percent injected dose per gram (% ID/g) relative to the injected dose. For receptor-blocking experiments U87MG tumor-bearing mice were scanned for the period 0–60 min p.i. after coinjection with radiotracer [^{18}F]6Glc-RGD or [^{18}F]Mlt-RGD (4–8 MBq) containing c(RGDfK) (12.5 mg/kg).

RESULTS

Chemistry. Based on our previous work on the comprehensive carbohydrate chemistry of glycosyl precursors, including **1a**,[20] we envisaged the synthesis of an extended series of glycosyl azides **1b–1f** bearing a tosylate leaving group for nucleophilic ^{18}F-substitution in 6-position of the carbohydrate (Figure 1). Employing classical synthetic methods, such as acetylation and deacetylation steps, fluorination by diethylaminosulfur trifluoride (DAST), and anomeric azido-for-bromo substitution reactions,[23−27] we achieved the synthesis of the labeling precursors **1b–1f**, following the route of the synthesis shown in Figure 2.

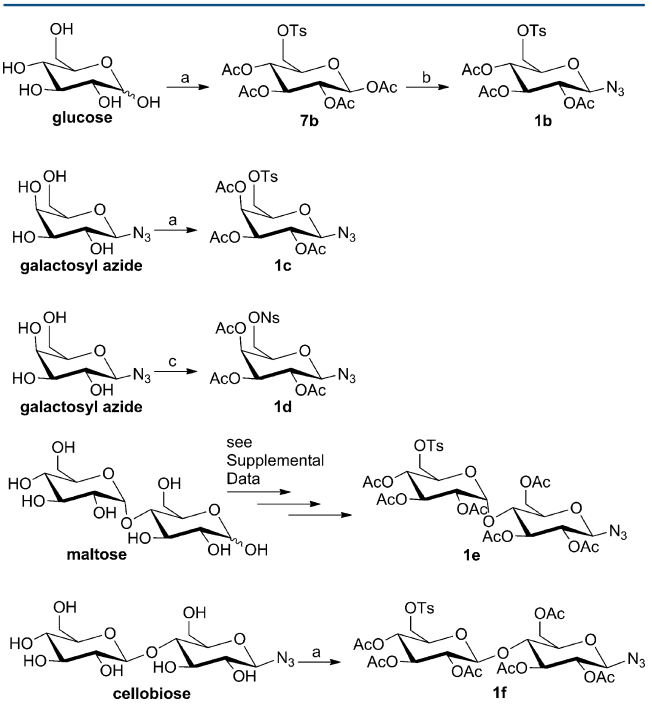

Figure 2. Course of the synthesis of ^{18}F-labeling precursors **1b–1f**. a: 1. TsCl, pyridine, 0 °C, 20 h, 2. Ac_2O, 1 h, 0 °C to rt; b: 1. HBr/AcOH, 0 °C to rt, 3 h, 2. NaN_3, tetrabutylammonium hydrogen sulfate, $NaHCO_3$, ethyl acetate, rt, 2 h; c: 1. NsCl, pyridine, 0 °C, 20 h, 2. Ac_2O, 1 h, 0 °C to rt. Please see the Supporting Information for details (Schemes S5 and S6).

Starting from the peracetylated glycosyl azides **2a–2f** and Zemplén deacetylation (Figure 3A), the corresponding free glycosyl azides **3a–3f** were reacted with the alkyne-bearing peptide c(RGDfPra) (Pra = propargyl glycine) by applying the chemoselective 1,3-dipolar cycloaddition under Cu(I)-catalyzed reaction conditions (click chemistry) as described previously.[21] Following this chemical strategy, the series of four RGD glycopeptides ^{19}F-6Glc-RGD (**4b**), ^{19}F-Gal-RGD (**4c**), ^{19}F-Mlt-RGD (**4e**), and ^{19}F-Cel-RGD (**4f**) were obtained in high yields of about 80% after preparative HPLC purification; their identity and purity (>98%) were proven by LC-ESI-MS.

Radiochemistry. The applicability of our new series of labeling precursors **1b**, **1c**, **1d**, **1e**, and **1f** for concomitant ^{18}F-labeling and glycosylation was investigated by applying a three-step two-pot labeling procedure, as depicted in Figure 4, following the strategy recently developed by our group for precursor **1a**.[20] The glucosyl 6-tosylate precursor **1b** gave the ^{18}F-labeled product [^{18}F]**2b** in 84 ± 7% radiochemical yield (RCY) after 10 min, whereas the galactosyl 6-nosylate

dx.doi.org/10.1021/mp4004817 | *Mol. Pharmaceutics* XXXX, XXX, XXX–XXX

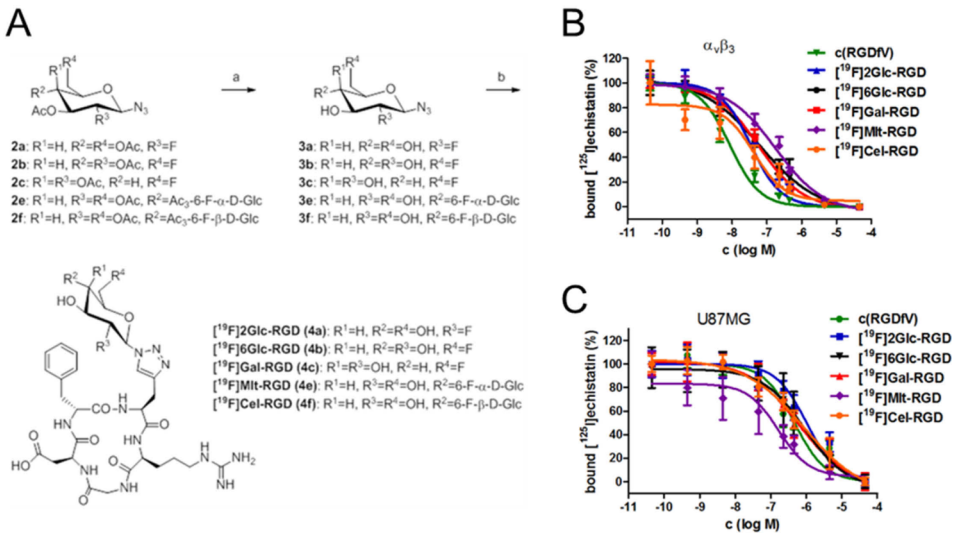

Figure 3. (A) Synthesis of the series of glycosylated RGD peptides **4a** (ref 21) and **4b**−**4f**. a: NaOMe, MeOH, rt, 1 h; b: c(RGDfPra), $CuSO_4$, sodium ascorbate, PBS/10% ethanol, rt, 30 min. (B) Displacement of [^{125}I]echistatin by RGD peptides using immobilized $\alpha_v\beta_3$. (C) Displacement of [^{125}I]echistatin by RGD peptides using U87MG cells. Each data point is the mean value ± SD from three independent experiments, each performed in triplicate.

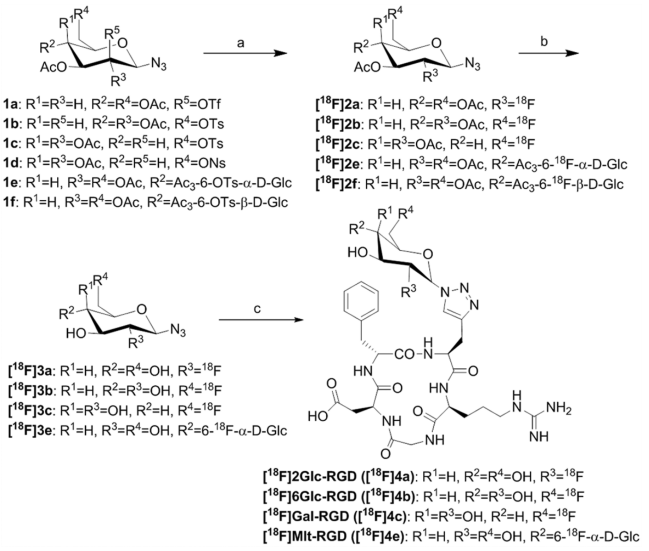

Figure 4. Radiosynthesis of ^{18}F-glyco-RGD peptides [^{18}F]6Glc-RGD, [^{18}F]Gal-RGD, and [^{18}F]Mlt-RGD. a: [$K^+ \subset$ K222]$^{18}F^-$, MeCN, 85 °C, 10 min; b: 60 mM NaOH, 60 °C, 5 min; c: c(RGDfPra), $CuSO_4$, sodium ascorbate, ethanol/water 1:1, 60 °C, 15−20 min.

precursor **1d** gave [^{18}F]**2c** in only 38 ± 8% RCY (Figure S1, Table S1). Notably, in case of the alternative galactosyl 6-tosyl-precursor **1c** an unidentified product occurred in radiochemical yields of 80%, whereas the desired product [^{18}F]**2c** had RCY of only 6 ± 3%. Alternative reaction parameters, such as the use of K_2CO_3 instead of K_2CO_3/KH_2PO_4, did not result in higher RCY (Table S1). The disaccharide precursors **1e** and **1f** were ^{18}F-labeled in RCYs of 61% and 6%, giving [^{18}F]**2e** and [^{18}F]**2f**, respectively. The low RCY of the cellobiosyl azide [^{18}F]**2f** prevented its use for the subsequent reactions. After semi-preparative HPLC isolation of the ^{18}F-labeled products [^{18}F]**2b**, [^{18}F]**2c**, or [^{18}F]**2e**, deacetylation was accomplished by the addition of sodium hydroxide (60 mM) to yield pure [^{18}F]**3b**, [^{18}F]**3c**, or [^{18}F]**3e**, respectively, after a reaction time of 5 min at 60 °C. These reaction conditions are very similar to those of the classical [^{18}F]FDG synthesis.[28,29] To investigate the potential of [^{18}F]**3b**, [^{18}F]**3c** or [^{18}F]**3c** as click labeling agents, the two-step one-pot approach was completed by neutralization and direct addition of the alkyne-functionalized c(RGDfPra) in the presence of copper(II)sulfate and sodium ascorbate. The RCY of this step was determined by analytical radio-HPLC being 81% for [^{18}F]6Glc-RGD ([^{18}F]**4b**), 36% for [^{18}F]Gal-RGD ([^{18}F]**4c**), and 80% for [^{18}F]Mlt-RGD ([^{18}F]**4e**) after 15−20 min at 60 °C (Figure S1, Table S1). After semi-preparative HPLC separation, the identity of ^{18}F-labeled compounds was verified by coinjection of the radiolabeled compounds together with the authentic ^{19}F-substituted compounds on an analytical HPLC system (Figure S2, Figure S3). [^{18}F]6Glc-RGD and [^{18}F]Mlt-RGD were obtained in an overall RCY of 16−24% (relative to [^{18}F]fluoride) in a total synthesis time of 70−75 min and in specific activities of 50−200 GBq/μmol. Due to their high-yielding and reliable radiosynthesis, we selected the glucosyl and the maltosyl RGD peptide ([^{18}F]6Glc-RGD and [^{18}F]Mlt-RGD) to proceed with a comparative *in vivo* study on the biodistribution and small-animal PET imaging.

***In Vitro* Studies.** *In Vitro Binding Assay for Glyco-RGD Peptides.* Integrin binding assays for [^{19}F]2Glc-RGD (**4a**) (only $\alpha_v\beta_5$; data on $\alpha_v\beta_3$ binding: see ref 21), [^{19}F]6Glc-RGD (**4b**), [^{19}F]Gal-RGD (**4c**), [^{19}F]Mlt-RGD (**4e**), and [^{19}F]Cel-RGD (**4f**) were performed as competition binding experiments using [^{125}I]echistatin as a radioligand and immobilized $\alpha_v\beta_3$, $\alpha_v\beta_5$, or $\alpha_v\beta_3$−positive U87MG cells, respectively, as described previously.[18] Notably, the $\alpha_v\beta_3$ integrin expression of U87MG cells was confirmed by immunofluorescence staining indicating $\alpha_v\beta_3$-positive and $\alpha_v\beta_5$-negative staining results (data not shown). The results of integrin binding affinities are presented in Table 1 and Figure 3B,C. As expected, all our RGD peptides inhibited the binding of [^{125}I]echistatin to $\alpha_v\beta_3$, $\alpha_v\beta_5$ and to U87MG cells in a concentration-dependent manner. The affinities of the glycosylated RGD peptides ranged from 11 to 55 nM for $\alpha_v\beta_3$, 6−14 nM for $\alpha_v\beta_5$ and 90−395 nM for U87MG cells. Interestingly, the glycosylation of c(RGDfPra) enhanced the binding affinity determined in U87MG cells by a

dx.doi.org/10.1021/mp4004817 | *Mol. Pharmaceutics* XXXX, XXX, XXX−XXX

Table 1. *In Vitro* Binding Affinities of a Series of RGD Glycopeptides and c(RGDfPra) and c(RGDfK) to $\alpha_v\beta_3$, $\alpha_v\beta_5$, and Human U87MG Cells (n = 3)[a]

compound	K_i ($\alpha_v\beta_3$)	K_i ($\alpha_v\beta_5$)	K_i (U87MG)
c(RGDfPra)	26 ± 6 nM[b]	13 ± 9 nM	1396 ± 365 nM[b]
4a: [^{19}F]2Glc-RGD	11 ± 4 nM[b]	8 ± 2 nM	395 ± 152 nM[b]
4b: [^{19}F]6Glc-RGD	31 ± 5 nM	7 ± 3 nM	287 ± 44 nM
4c: [^{19}F]-Gal-RGD	22 ± 4 nM	14 ± 9 nM	270 ± 150 nM
4e: [^{19}F]Mlt-RGD	55 ± 14 nM	6 ± 2 nM	90 ± 45 nM
4f: [^{19}F]Cel-RGD	30 ± 6 nM	n.d.	228 ± 33 nM
c(RGDfK)	32 ± 8 nM	12 ± 7 nM	n.d.

[a]Data are expressed as mean values ± standard deviation from three independent experiments, each determined in triplicate; n.d. = not determined. [b]Values from ref 21 for comparison.

factor of 15 in the case of the maltosyl peptide [^{19}F]Mlt-RGD relative to the nonglycosylated parent compound c(RGDfPra) (Table 1).

Lipophilicity and Stability in Serum of the RGD Glycopeptides in Vitro. The log $D_{7.4}$ values of the glycosylated RGD peptides are listed in Table 2. The disaccharyl peptide

Table 2. Log $D_{7.4}$ Values of the Various Glycosylated RGD Peptides[a]

compound	log $D_{7.4}$
[^{18}F]2Glc-RGD	−3.77 ± 0.22[b]
[^{18}F]6Glc-RGD	−3.47 ± 0.13
[^{18}F]Gal-RGD	−3.56 ± 0.07
[^{18}F]Mlt-RGD	−4.10 ± 0.12

[a]Data are expressed as mean values ± standard deviation from 3 independent experiments. [b]Values from ref 21 for comparison.

[^{18}F]Mlt-RGD was slighty more hydrophilic than the RGD peptides coupled to the monosaccharides glucose ([^{18}F]2Glc-RGD, [^{18}F]6Glc-RGD) and galactose ([^{18}F]Gal-RGD). The high stability of cyclic RGD peptides in serum is well-known. We confirmed the stability of [^{18}F]6Glc-RGD and [^{18}F]Mlt-RGD in human serum *in vitro* at 37 °C (Figures S6 and S7). Both radiotracers did not show any degradation within 60 min as determined by analytical radio-HPLC.

***In Vivo* Studies.** *Biodistribution and Small-Animal PET Imaging in Tumor-Bearing Nude Mice.* The biodistribution studies were performed with [^{18}F]6Glc-RGD and [^{18}F]Mlt-RGD using U87MG tumor bearing nude mice, and results are shown in Table 3 and Table 4 (see also Figure S4). Both radiotracers showed a similar tumor uptake of 0.8%ID/g after 60 min p.i. (Figure 5A). At 120 min p.i. [^{18}F]Mlt-RGD showed a higher retention in the tumor than did [^{18}F]6Glc-RGD (0.8 vs 0.3%ID/g, respectively). Both radiotracers displayed specific tumor uptake as determined by coinjection of radiotracer with the blocker c(RGDfK) (Table 3, Table 4, Figure S5). The radioactivity concentrations in normal organs 60 min p.i. were similarly expected for kidney and liver; [^{18}F]Mlt-RGD had 40% lower renal uptake at 60 min post injection and 61% lower hepatic uptake. [^{18}F]6Glc-RGD showed fast clearance from the blood and most examined organs, whereas [^{18}F]Mlt-RGD showed a significantly decreased clearance from blood and higher retention in most organs compared to [^{18}F]6Glc-RGD (see Figure S4). This led to higher tumor-to-blood values for [^{18}F]6Glc-RGD than for [^{18}F]Mlt-RGD (Figure 5B), whereas tumor-to-muscle ratios were similar (Figure 5B) and tumor-to-

Table 3. Biodistribution Data for [^{18}F]6Glc-RGD ([^{18}F]4b) Measured in U87MG Bearing Nude Mice[a]

organ	30 min	65 min	65 min blocking[b]	120 min
blood	0.50 ± 0.32	0.09 ± 0.04	0.04 ± 0.01	0.04 ± 0.01
lung	0.80 ± 0.17	0.43 ± 0.05	0.12 ± 0.02	0.23 ± 0.05
liver	3.65 ± 0.45	2.46 ± 0.29	2.19 ± 0.36	1.33 ± 0.23
kidney	4.53 ± 1.63	1.69 ± 0.62	2.23 ± 0.49	1.07 ± 0.12
heart	0.32 ± 0.10	0.26 ± 0.22	0.05 ± 0.02	0.10 ± 0.04
spleen	0.63 ± 0.08	0.49 ± 0.26	0.10 ± 0.06	0.27 ± 0.10
U87MG tumor	1.33 ± 0.43	0.79 ± 0.32	0.11 ± 0.03	0.33 ± 0 07
brain	0.07 ± 0.02	0.07 ± 0.04	0.06 ± 0.05	0.02 ± 0 01
muscle	1.06 ± 0.70	0.68 ± 0.32	1.41 ± 1.29	0.29 ± 0.34
intestine	1.25 ± 0.74	0.60 ± 0.36	2.29 ± 2.68	0.96 ± 0.99
femur	0.51 ± 0.40	0.23 ± 0.23	0.13 ± 0.12	0.15 ± 0.06

[a]Data represent mean values ± standard deviation (n = 3−4). [b]Coinjection of 12.5 mg/kg c(RGDfK).

kidney and tumor-to-liver values were higher for [^{18}F]Mlt-RGD by about a factor of 2 (Figure S4).

In small-animal PET studies with U87MG tumor-bearing mice, [^{18}F]6Glc-RGD and [^{18}F]Mlt-RGD were compared to [^{18}F]2Glc-RGD. The two novel tracers had similar time-activity-curves SUV units (Figure 6). PET recordings for [^{18}F]6Glc-RGD and [^{18}F]Mlt-RGD mirrored the biodistribution data at 60 min p.i., with almost equal tumor uptake (Figure S5), which gave adequate tumor visualization. In animals coinjected with radiotracer and c(RGDfK), tumor uptake was negligible, demonstrating the specificity of both [^{18}F]6Glc-RGD and [^{18}F]Mlt-RGD for imaging of integrin expression *in vivo* by PET (Figure 6A−F).

DISCUSSION

We investigated the influence of different glycosyl moieties on the biodistribution and clearance pattern of cyclic RGD pentapeptides. To this end we synthesized five tosyl or nosyl containing glycosyl-azides as ^{18}F-labeling precursors and examined the binding of the corresponding series of fluoroglycosyl peptides *in vitro* and the biodistribution properties *in vivo*. The synthesis of the labeling precursors were easily achieved by reaction of glucose, galactosylazide, maltosyl azide, or cellobiosyl azide, respectively, with tosyl or nosyl chloride in pyridine and subsequent acetylation using acetic anhydride.[23] After column chromatography, the labeling precursors were obtained as pure β-anomers. The ^{18}F-labeling was performed using mild reaction conditions with a lower amount of K_2CO_3 in the presence of KH_2PO_4 compared to commonly used ^{18}F-labeling conditions.[28,30] This modification proved to be advantageous for the subsequent separation of the ^{18}F-labeled products by semipreparative HPLC,[20] in that the less basic reaction medium resulted in less elimination reactions and degradation of the labeling precursors.

In our initial proof-of-principle of the present concept, [^{18}F]2Glc-RGD displayed relatively high uptake in liver (4.8% ID/g) and kidney (6.6%ID/g) at 120 min postinjection.[21] Moving the ^{18}F-label in the glucosyl residue from position 2 to position 6 in the present study led to significantly reduced kidney and liver uptake of [^{18}F]6Glc-RGD (1.1%ID/g and 1.3%ID/g, respectively). Since the log $D_{7.4}$ values for [^{18}F]6Glc-RGD and [^{18}F]2Glc-RGD as well as their *in vitro* binding properties are very similar, this favorable effect is most likely

dx.doi.org/10.1021/mp4004817 | *Mol. Pharmaceutics* XXXX, XXX, XXX−XXX

Table 4. Biodistribution Data for [^{18}F]Mlt-RGD ([^{18}F]4e) Measured in U87MG Bearing Nude Mice[a]

organ	30 min	60 min	60 min blocking[b]	120 min
blood	0.36 ± 0.10	0.27 ± 0.01	0.08 ± 0.02	0.29 ± 0.04
lung	0.85 ± 0.10	0.50 ± 0.05	0.17 ± 0.02	0.45 ± 0.06
liver	1.00 ± 0.06	0.95 ± 0.06	0.39 ± 0.08	0.83 ± 0.15
kidney	1.76 ± 0.43	1.01 ± 0.05	0.59 ± 0.16	0.83 ± 0.16
heart	0.33 ± 0.03	0.25 ± 0.02	0.05 ± 0.01	0.27 ± 0.03
spleen	0.56 ± 0.04	0.45 ± 0.02	0.12 ± 0.09	0.43 ± 0.06
U87MG tumor	1.26 ± 0.14	0.85 ± 0.11	0.09 ± 0.02	0.76 ± 0.15
brain	0.12 ± 0.01	0.14 ± 0.01	0.02 ± 0.01	0.22 ± 0.04
muscle	0.24 ± 0.04	0.30 ± 0.13	0.41 ± 0.38	0.22 ± 0.05
intestine	0.69 ± 0.11	0.57 ± 0.11	0.25 ± 0.27	0.44 ± 0.02
femur	0.32 ± 0.09	0.28 ± 0.07	0.23 ± 0.17	0.24 ± 0.03
pancreas	0.29 ± 0.06	0.19 ± 0.03	0.17 ± 0.16	0.20 ± 0.04
duodenum	0.92 ± 0.05	0.72 ± 0.17	0.18 ± 0.07	0.61 ± 0.13

[a]Data represent mean values ± standard deviation (n = 3–4). [b]Coinjection of 12.5 mg/kg c(RGDfK).

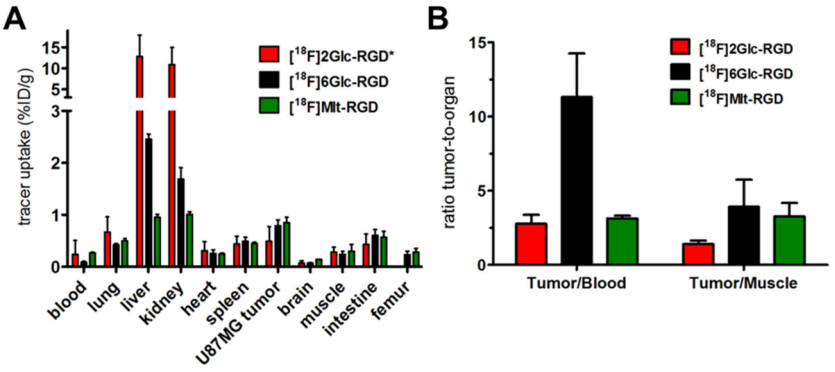

Figure 5. Biodistribution data (A) and tumor-to-organ ratios (B) of [^{18}F]2Glc-RGD, [^{18}F]6Glc-RGD, and [^{18}F]Mlt-RGD in nude mice bearing U87MG tumors 60 min p.i. Data are expressed as mean values ± SD from 3 to 5 animals. *Data of [^{18}F]2Glc-RGD are taken from ref 21 and depicted for comparison.

due to differences in the metabolic fate of the tracers *in vivo*. We can speculate that the formation of the glucuronic acid by oxidation in the 6-position in the liver could result in high liver uptake of radioactivity from [^{18}F]2Glc-RGD, whereas the oxidative trapping would not be possible in the case of [^{18}F]6Glc-RGD.

A variety of ^{18}F-labeled RGD peptides have been synthesized during the past decade.[3] One radioactive RGD peptide which already finds frequent clinical use is [^{18}F]Galacto-RGD, which was developed by Haubner et al. in 2001.[9] Its use is encouraged by the favorable pharmacokinetics of this glycopeptide. In contrast to the large variety of other radiolabeled RGD derivatives containing bulky aromatic groups (e.g., [^{18}F]SFB or [^{18}F]FBA), [^{18}F]GalactoRGD is a glycoconjugate, making it a hydrophilic tracer with fast blood clearance and predominantly renal excretion *in vivo*. However, a major drawback of [^{18}F]Galacto-RGD is the time-consuming four-step radiosythesis with an overall preparation time of 200 min, which includes three HPLC separations.[8] In contrast, the RGD glycopeptides presented in this study are prepared by efficient and simple click-chemistry. Our new radiosythesis consists of a three-step (two-pot) procedure and includes two HPLC separations, saving at least 120 min in the overall preparation time, which equals one-half life of fluorine-18, and thus resulting in a significantly increased radiochemical yield of the ^{18}F-labeled glycopeptides.

Our results of the biodistribution of [^{18}F]Mlt-RGD are very similar to that reported for [^{18}F]Galacto-RGD.[9,31] Comparing [^{18}F]Mlt-RGD to [^{18}F]Galacto-RGD in the U87MG nude mice model, the tumor-to-kidney-ratio, the tumor-to-liver-ratio, and the total tumor uptake at 120 min p.i. were almost equal (0.9% ID/g).[31] However, [^{18}F]Mlt-RGD reached the peak value of 0.9%ID/g much earlier, at only 60 min post injection. The uptake for [^{18}F]Galacto-RGD in the M21 tumor model is reportedly twice as high as that of [^{18}F]Mlt-RGD in U87MG tumors.[9] This difference could be most likely ascribed to differences in the overall $\alpha_v\beta_3$ or $\alpha_v\beta_5$ integrin expression between the M21 tumors and U87MG tumors, as [^{18}F]Galacto-RGD showed similar uptake in U87MG tumors when compared with [^{18}F]Mlt-RGD.[31]

The tumor-to-blood ratio for [^{18}F]Galacto-RGD at 120 min p.i. is reported to be 30,[9] while [^{18}F]6Glc-RGD gave a ratio of 8 and [^{18}F]Mlt-RGD only 3 (Figure 5B). The lower ratio of [^{18}F]Mlt-RGD is due to its relatively slow blood clearance between 30 and 120 min p.i. as compared with the glucosyl analogue (Table 4; Figure S4). The hydrophilicities of [^{18}F]Mlt-RGD and [^{18}F]6Glc-RGD are comparable (log $D_{7.4}$ of −3.5 vs. −4.1), with [^{18}F]Mlt-RGD having the highest hydrophilicity in the series of glycopeptides under study. Thus, hydrophobicity gives no direct explanation for the apparently slow blood clearance of [^{18}F]Mlt-RGD. However, a similar effect of glycosylation on blood clearance was found by Schottelius et al. for ^{125}I-iodinated glycosylated octreotide derivatives, where elongation of the glucose moiety from a monosaccharide to a trisaccharide chain decreased the tumor-to-blood ratio from 6 to 2.[32]

dx.doi.org/10.1021/mp4004817 | Mol. Pharmaceutics XXXX, XXX, XXX–XXX

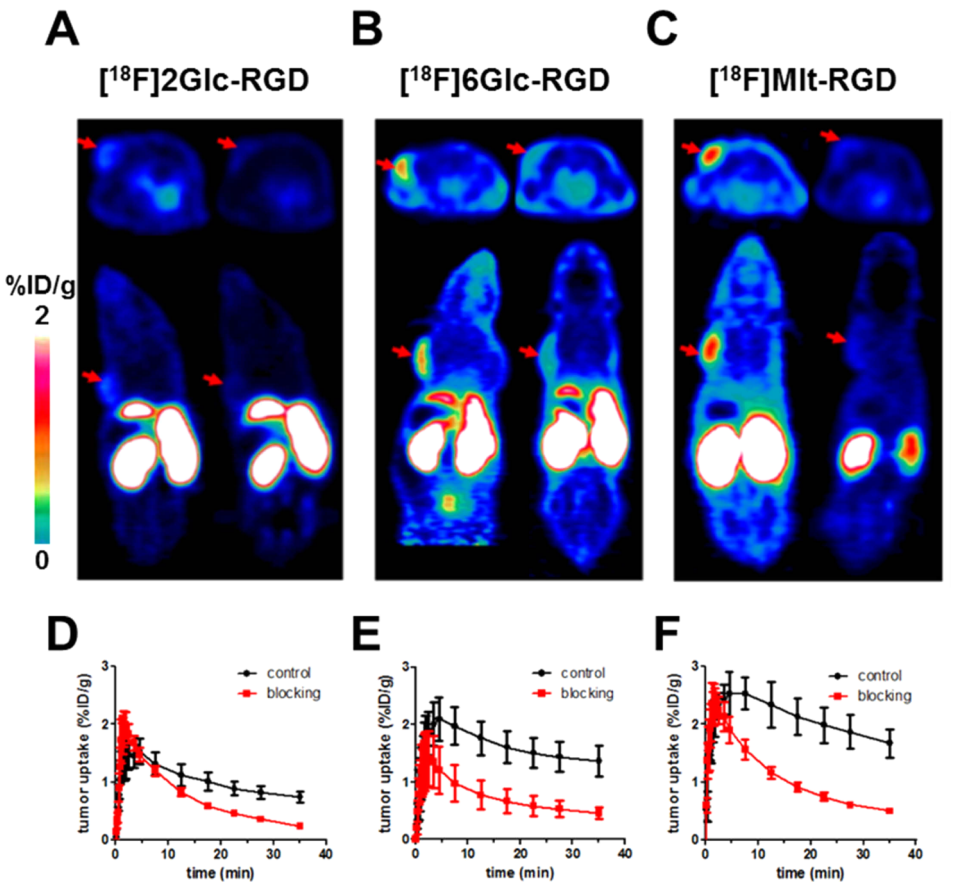

Figure 6. Small-animal PET using [^{18}F]2Glc-RGD (A), [^{18}F]6Glc-RGD (B), and [^{18}F]Mlt-RGD (C) at 60 min p.i.: Transaxial (top) and coronal (bottom) images from U87MG-bearing mice injected with the tracer alone (control, left) and coinjection of c(RGDfK) (12.5 mg/kg, blocking, right). (D–F) Time–activity curves of dynamic small-animal PET acquisitions. Data represent mean values ± SD from 3 to 5 animals.

Multimeric RGD peptides have the principle advantage of higher tumor uptake and high tumor retention and sufficient clearance properties for imaging purposes, as recently been demonstrated by various studies.[33−35] Among these, Guo et al. recently reported the comparison of three dimeric ^{18}F-AlF-NOTA-RGD tracers, demonstrating tumor uptake values of 2.1−2.8%ID/g in U87MG xenografts, liver uptake of 1.6−2.0% ID/g, and kidney uptake of 2.0−2.6%ID/g at 120 min postinjection.[35] Furthermore, the recently reported ^{18}F-labeled dimeric RGD peptide [c(RGDfK)]$_2$E-^{18}F-ArBF$_3^-$ showed rather low tumor uptake of 0.5%ID/g in U87MG tumor-bearing nude mice.[36] The authors ascribed this result to the marked renal clearance of the tracer.

With [^{18}F]Mlt-RGD we found a tumor uptake of approximately 1% ID/g at 120 min p.i., being lower than that of most dimeric RGD tracers, but significantly higher than the tumor uptake of the dimeric RGD peptide [c(RGDfK)]$_2$E-^{18}F-ArBF$_3^-$.[36] Moreover, the uptake values of [^{18}F]Mlt-RGD in liver and kidney were desirably low (both 0.8%ID/g) compared to the dimeric tracers reported by Guo et al. (1.6−2.6%ID/g;[35] see above). Notably, the low kidney uptake of [^{18}F]Mlt-RGD resulted in a tumor/kidney ratio of 1, very closely reflecting the tumor/kidney ratio of the dimeric RGD peptides reported by Guo and co-workers (1.02−1.06).[35] Therefore, dimeric RGD peptides show higher tumor uptake which is consistent with the general theory of improved avidities of multimeric ligands to the $\alpha_v\beta_3$ integrin,[33] whereas the fluoroglycosylation method, in the case of [^{18}F]Mlt-RGD, induced a suitable balance between improved renal clearance and sufficient tumor uptake in combination with a relatively high tumor retention of 60% (120 min p.i. vs 30 min p.i., Table 4), resulting in tumor/background ratios similar to those of dimeric peptides.

Taken together, in this study of fluoroglycosylation of a cyclic RGD peptide we indentified two glycopeptide tracers, namely, [^{18}F]6Glc-RGD and [^{18}F]Mlt-RGD, which were prepared by the same radiochemical procedure, but with greatly different pharmacokinetic properties *in vivo*. Both radiotracers showed a dramatic decrease in kidney and liver uptake when compared with the previously published [^{18}F]2Glc-RGD.[21] While [^{18}F]6Glc-RGD has favorable tumor-to-blood ratios in the U87MG tumor model, but only low tumor retention, [^{18}F]Mlt-RGD proved to have slower blood clearance but even less uptake in the kidney and liver. These properties, in conjunction with high tumor retention, make [^{18}F]Mlt-RGD a promising candidate for molecular studies of the integrin expression.

CONCLUSION

The aim of this study was to develop an alternative radiopharmaceutical for the clinically used tracer [^{18}F]-Galacto-RGD for the noninvasive determination of the $\alpha_v\beta_3$ expression. To this end we extended our previously designed radiosynthesis method based on the CuAAC click chemistry, using different ^{18}F-glycosyl azides and an alkyne-bearing RGD peptide. Our approach generalized to a reliable and high-yielding ^{18}F-synthetic strategy. The series of new ^{18}F-fluoroglycosylated RGD peptides displayed high affinity toward

dx.doi.org/10.1021/mp4004817 | *Mol. Pharmaceutics* XXXX, XXX, XXX−XXX

the integrins $\alpha_v\beta_3$ and $\alpha_v\beta_5$ and showed distinct *in vivo* properties. Compared to [^{18}F]Galacto-RGD, [^{18}F]Mlt-RGD has similar tumor-to-background values, resulting from a predominantly renal clearance together with high tumor retention. Thus, [^{18}F]Mlt-RGD is distinguished by a favorable *in vivo* biodistribution, while presenting benefits over [^{18}F]-Galacto-RGD imparted by more rapid and simplified radiosynthesis, thus representing a very promising alternative radiotracer for imaging integrin expression by PET in further (pre)clinical studies.

■ ASSOCIATED CONTENT

Supporting Information

General information on Materials and Methods. Syntheses of **1e**, **1f**, **2b**, **2c**, **2e**, **2f**, **3c**, **3e**, **3f**, **5e**, **7e**, **8e**, **9e**, **10e**, **11e**; Schemes S1−S6. Radiochemical yields (RCY) of the two-step glycosylation reaction; Table S1. Radiochemical yields of the ^{18}F-labeled glycosyl azides [^{18}F]**2a−f**; Figure S1A. Time dependency of the RCY of the RGD glycopeptides [^{18}F]**4a−c** and [^{18}F]**4e** for the glycosylation reaction step; Figure S1B. HPLC analysis of [^{18}F]6Glc-RGD (radiochemical identity); Figure S2. HPLC analysis of [^{18}F]Mlt-RGD (radiochemical identity); Figure S3. Biodistribution data of [^{18}F]6Glc-RGD and [^{18}F]Mlt-RGD in U87MG tumor-bearing nude mice 30, 60, and 120 min p.i.; Figure S4. Tumor uptake of [^{18}F]2Glc-RGD ([^{18}F]**4a**[21]) in comparison with [^{18}F]6Glc-RGD ([^{18}F]**4b**) and [^{18}F]Mlt-RGD ([^{18}F]**4e**) in U87MG tumor-bearing nude mice at 60 min postinjection; Figure S5. Stability of [^{18}F]6Glc-RGD and [^{18}F]Mlt-RGD in human serum in vitro; Figures S6 and S7. This material is available free of charge via the Internet at http://pubs.acs.org.

■ AUTHOR INFORMATION

Corresponding Author

*Molecular Imaging and Radiochemistry, Nuclear Medicine Clinic, Friedrich-Alexander University, Schwabachanlage 6, D-91054 Erlangen, Germany. Tel.: +49-9131-8544440. Fax: +49-9131-8534440. E-mail: olaf.prante@uk-erlangen.de.

Notes

The authors declare no competing financial interest.

■ ACKNOWLEDGMENTS

The authors thank Bianca Weigel, Susanne Knauf, and Dr. Carsten Hocke for expert technical support and thank Dr. Paul Cumming for critical revisions to the manuscript. This work was supported by the Deutsche Forschungsgemeinschaft (DFG, grants MA 4295/1-2 and PR 677/5-1).

■ REFERENCES

(1) Folkman, J. Angiogenesis: an organizing principle for drug discovery? *Nat. Rev. Drug Discovery* **2007**, *6*, 273−286.

(2) Al-Husein, B.; Abdalla, M.; Trepte, M.; Deremer, D. L.; Somanath, P. R. Antiangiogenic therapy for cancer: an update. *Pharmacotherapy* **2012**, *32*, 1095−1111.

(3) Haubner, R.; Beer, A. J.; Wang, H.; Chen, X. Positron emission tomography tracers for imaging angiogenesis. *Eur. J. Nucl. Med. Mol. Imaging* **2010**, *37*, S86−S103.

(4) Aumailley, M.; Gurrath, M.; Muller, G.; Calvete, J.; Timpl, R.; Kessler, H. Arg-Gly-Asp constrained within cyclic pentapeptides. Strong and selective inhibitors of cell adhesion to vitronectin and laminin fragment P1. *FEBS Lett.* **1991**, *291*, 50−54.

(5) Schottelius, M.; Laufer, B.; Kessler, H.; Wester, H.-J. Ligands for Mapping $\alpha_v\beta_3$-Integrin Expression in Vivo. *Acc. Chem. Res.* **2009**, *42*, 969−980.

(6) Wan, W.; Guo, N.; Pan, D.; Yu, C.; Weng, Y.; Luo, S.; Ding, H.; Xu, Y.; Wang, L.; Lang, L.; Xie, Q.; Yang, M.; Chen, X. First Experience of ^{18}F-Alfatide in Lung Cancer Patients Using a New Lyophilized Kit for Rapid Radiofluorination. *J. Nucl. Med.* **2013**, *54*, 691−698.

(7) Beer, A. J.; Schwaiger, M. PET imaging of a_vb_3 expression in cancer patients. *Methods Mol. Biol.* **2011**, *680*, 183−200.

(8) Haubner, R.; Kuhnast, B.; Mang, C.; Weber, W. A.; Kessler, H.; Wester, H. J.; Schwaiger, M. [^{18}F]Galacto-RGD: synthesis, radiolabeling, metabolic stability, and radiation dose estimates. *Bioconjugate Chem.* **2004**, *15*, 61−69.

(9) Haubner, R.; Wester, H. J.; Weber, W. A.; Mang, C.; Ziegler, S. I.; Goodman, S. L.; Senekowitsch-Schmidtke, R.; Kessler, H.; Schwaiger, M. Noninvasive imaging of $\alpha_v\beta_3$ integrin expression using ^{18}F-labeled RGD-containing glycopeptide and positron emission tomography. *Cancer Res.* **2001**, *61*, 1781−1785.

(10) Schottelius, M.; Rau, F.; Reubi, J. C.; Schwaiger, M.; Wester, H. A. Modulation of pharmacokinetics of radioiodinated sugar-conjugated somatostatin analogues by variation of peptide net charge and carbohydration chemistry. *Bioconjugate Chem.* **2005**, *16*, 429−437.

(11) Fischer, C. R.; Müller, C.; Reber, J.; Müller, A.; Kramer, S. D.; Ametamey, S. M.; Schibli, R. [^{18}F]Fluoro-Deoxy-Glucose Folate: A Novel PET Radiotracer with Improved in Vivo Properties for Folate Receptor Targeting. *Bioconjugate Chem.* **2012**, *23*, 805−813.

(12) Kolb, H. C.; Finn, M. G.; Sharpless, K. B. Click Chemistry: Diverse Chemical Function from a Few Good Reactions. *Angew. Chem., Int. Ed. Engl.* **2001**, *40*, 2004−2021.

(13) Rostovtsev, V. V.; Green, L. G.; Fokin, V. V.; Sharpless, K. B. A stepwise Huisgen cycloaddition process: Copper(I)-catalyzed regioselective "ligation" of azides and terminal alkynes. *Angew. Chem., Int. Ed.* **2002**, *41*, 2596−2599.

(14) Tornoe, C. W.; Christensen, C.; Meldal, M. Peptidotriazoles on solid phase: [1,2,3]-triazoles by regiospecific copper(I)-catalyzed 1,3-dipolar cycloadditions of terminal alkynes to azides. *J. Org. Chem.* **2002**, *67*, 3057−3064.

(15) Namavari, M.; Cheng, Z.; Zhang, R.; De, A.; Levi, J.; Hoerner, J. K.; Yaghoubi, S. S.; Syud, F. A.; Gambhir, S. S. A Novel Method for Direct Site-Specific Radiolabeling of Peptides Using [^{18}F]FDG. *Bioconjugate Chem.* **2009**, *20*, 432−436.

(16) Hultsch, C.; Schottelius, M.; Auernheimer, J.; Alke, A.; Wester, H. J. ^{18}F-Fluoroglucosylation of peptides, exemplified on cyclo-(RGDfK). *Eur. J. Nucl. Med. Mol. Imaging* **2009**, *36*, 653−658.

(17) Schottelius, M.; Poethko, T.; Herz, M.; Reubi, J. C.; Kessler, H.; Schwaiger, M.; Wester, H. J. First ^{18}F-labeled tracer suitable for routine clinical imaging of sst receptor-expressing tumors using positron emission tomography. *Clin. Cancer Res.* **2004**, *10*, 3593−3606.

(18) Prante, O.; Einsiedel, J.; Haubner, R.; Gmeiner, P.; Wester, H. J.; Kuwert, T.; Maschauer, S. 3,4,6-tri-O-acetyl-2-deoxy-2-[^{18}F]-fluoroglucopyranosyl phenylthiosulfonate: A thiol-reactive agent for the chemoselective ^{18}F-glycosylation of peptides. *Bioconjugate Chem.* **2007**, *18*, 254−262.

(19) Wuest, F.; Berndt, M.; Bergmann, R.; van den Hoff, J.; Pietzsch, J. Synthesis and application of [^{18}F]FDG-maleimidehexyloxime ([^{18}F]FDG-MHO): A [^{18}F]FDG-based prosthetic group for the chemoselective ^{18}F-labeling of peptides and proteins. *Bioconjugate Chem.* **2008**, *19*, 1202−1210.

(20) Maschauer, S.; Prante, O. A series of 2-*O*-trifluoromethylsulfonyl-D-mannopyranosides as precursors for concomitant ^{18}F-labeling and glycosylation by click chemistry. *Carbohydr. Res.* **2009**, *344*, 753−761.

(21) Maschauer, S.; Einsiedel, J.; Haubner, R.; Hocke, C.; Ocker, M.; Hübner, H.; Kuwert, T.; Gmeiner, P.; Prante, O. Labeling and Glycosylation of Peptides Using Click Chemistry: A General Approach to ^{18}F-Glycopeptides as Effective Imaging Probes for Positron Emission Tomography. *Angew. Chem., Int. Ed.* **2010**, *49*, 976−979.

(22) Boutureira, O.; Bernardes, G. J. L.; D'Hooge, F.; Davis, B. G. Direct radiolabelling of proteins at cysteine using [^{18}F]-fluorosugars. *Chem. Commun.* **2011**, *47*, 10010−10012.
(23) Gyoergydeak, Z.; Szilagyi, L. Facile Syntheses of galactopyranosyl and glucopyranosyl azides substituted at C-6. *Liebigs Ann. Chem.* **1987**, 235−241.
(24) Lopez, M.; Trajkovic, J.; Bornaghi, L. F.; Innocenti, A.; Vullo, D.; Supuran, C. T.; Poulsen, S. A. Design, Synthesis, and Biological Evaluation of Novel Carbohydrate-Based Sulfamates as Carbonic Anhydrase Inhibitors. *J. Med. Chem.* **2011**, *54*, 1481−1489.
(25) Porwanski, S.; Marsura, A. Tandem Staudinger-Aza-Wittig Templated Reaction: De Novo Synthesis of Sugar-Ureido Cryptands. *Eur. J. Org. Chem.* **2009**, 2047−2050.
(26) Schengrund, C. L.; Kovac, P. UDP-6-deoxy-6-fluoro-a-D-galactose binds to two different galactosyltransferases, but neither can effectively catalyze transfer of the modified galactose to the appropriate acceptor. *Carbohydr. Res.* **1999**, *319*, 24−28.
(27) Withers, S. G.; MacLennan, D. J.; Street, I. P. The synthesis and hydrolysis of a series of deoxyfluoro-D-glucopyranosyl phosphates. *Carbohydr. Res.* **1986**, *154*, 127−144.
(28) Hamacher, K.; Coenen, H. H.; Stöcklin, G. Efficient stereospecific synthesis of no-carrier-added 2-[^{18}F]-fluoro-2-deoxy-D-glucose using aminopolyether supported nucleophilic substitution. *J. Nucl. Med.* **1986**, *27*, 235−238.
(29) Füchtner, F.; Steinbach, J.; Mäding, P.; Johannsen, B. Basic hydrolysis of 2-[^{18}F]fluoro-1,3,4,6-tetra-O-acetyl-d-glucose in the preparation of 2-[^{18}F]fluoro-2-deoxy-d-glucose. *Appl. Radiat. Isot.* **1996**, *47*, 61−66.
(30) Coenen, H. H.; Schüller, M.; Stöcklin, G.; Klatte, B.; Knöchel, A. Preparation of N.C.A. [17-^{18}F]-fluoroheptadecanoic acid in high yields via aminopolyether supported, nucleophilic fluorination. *J. Label. Compds. Radiopharm.* **1986**, *23*, 455−466.
(31) Liu, S.; Liu, Z.; Chen, K.; Yan, Y.; Watzlowik, P.; Wester, H. J.; Chin, F. T.; Chen, X. ^{18}F-labeled galacto and PEGylated RGD dimers for PET imaging of $\alpha_v\beta_3$ integrin expression. *Mol. Imaging Biol.* **2010**, *12*, 530−538.
(32) Schottelius, M.; Wester, H. J.; Reubi, J. C.; Senekowitsch-Schmidtke, R.; Schwaiger, M. Improvement of pharmacokinetics of radioiodinated Tyr^3-octreotide by conjugation with carbohydrates. *Bioconjugate Chem.* **2002**, *13*, 1021−1030.
(33) Liu, S. Radiolabeled cyclic RGD peptides as integrin $\alpha_v\beta_3$-targeted radiotracers: maximizing binding affinity via bivalency. *Bioconjugate Chem.* **2009**, *20*, 2199−2213.
(34) Wängler, C.; Maschauer, S.; Prante, O.; Schafer, M.; Schirrmacher, R.; Bartenstein, P.; Eisenhut, M.; Wängler, B. Multimerization of cRGD peptides by click chemistry: synthetic strategies, chemical limitations, and influence on biological properties. *ChemBioChem* **2010**, *11*, 2168−2181.
(35) Guo, J.; Lang, L.; Hu, S.; Guo, N.; Zhu, L.; Sun, Z.; Ma, Y.; Kiesewetter, D. O.; Niu, G.; Xie, Q.; Chen, X. Comparison of Three Dimeric F-AlF-NOTA-RGD Tracers. *Mol. Imaging Biol.* **2013**, 10.1007/s11307-013-0668-1.
(36) Li, Y.; Liu, Z.; Lozada, J.; Wong, M. Q.; Lin, K. S.; Yapp, D.; Perrin, D. M. Single step F-labeling of dimeric cycloRGD for functional PET imaging of tumors in mice. *Nucl. Med. Biol.* **2013**, *40*, 959−966.